Information systems research

UDC 004.932 **doi:** https://doi.org/10.20998/2522-9052.2024.2.06

Artem Hurin[1], Hennadii Khudov[1], Oleksandr Kostyria[1], Oleh Maslenko[2], Serhii Siadrystyi[1]

[1] Ivan Kozhedub Kharkiv National Air Force University, Kharkiv, Ukraine
[2] Defence Intelligence Research Institute, Kyiv, Ukraine

COMPARATIVE ANALYSIS OF SPECTRAL ANOMALIES DETECTION METHODS ON IMAGES FROM ON-BOARD REMOTE SENSING SYSTEMS

Abstract. The **subject matter** of the article is methods of detecting spectral anomalies on images from remote sensing systems. The **goal** is to conduct a comparative analysis of methods for detecting spectral anomalies on images from remote sensing systems. The **tasks** are: analysis of the main methods of detecting spectral anomalies on images from remote sensing systems; processing of images from remote sensing systems using basic methods of detecting spectral anomalies; comparative assessment of the quality of methods for detecting spectral anomalies on images from remote monitoring systems. The **methods** used are: methods of digital image processing, mathematical apparatus of matrix theory, methods of mathematical modeling, methods of optimization theory, analytical and empirical methods of image comparison. The following **results** are obtained. The main methods of detecting spectral anomalies on images from remote sensing systems were analyzed. Processing of images from remote sensing systems using the basic methods of detecting spectral anomalies was carried out. A comparative assessment of the quality of methods for detecting spectral anomalies on images from remote monitoring systems was carried out. **Conclusions**. The spectral difference of the considered methods is revealed by the value of information indicators - Euclidean distance, Mahalanobis distance, brightness contrast, and Kullback-Leibler information divergence. Mathematical modeling of the considered methods of detecting spectral anomalies of images with a relatively "simple" and complicated background was carried out. It was established that when searching for a spectral anomaly on an image with a complicated background, the method based on the Kullback-Leibler divergence can be more effective than the other considered methods, but is not optimal. When determining several areas of the image with high divergence indicators, they should be additionally investigated using the specified methods in order to more accurately determine the position of the spectral anomaly.

Keywords: spectral anomaly; detection; remote sensing; imaging; Mahalanobis distance; brightness contrast; Kullback-Leibler divergence.

Introduction

Formulation of the problem. Systems of remote sensing of the Earth provide wide opportunities for both operational shooting and accumulation of data archives [1].

So, for example, space systems for remote sensing of the Earth have the ability to receive images of the land and water surface under different observation conditions (time of year, day, cloud cover, etc.). The information received from Earth remote sensing satellites is used in the following areas [1, 2]: agriculture, land use, forestry, control of water resources, observation of coastal zones and oceans, climatology, control of global atmospheric phenomena, meteorology, geodesy, cartography, urban planning, search for minerals and energy sources, emergency monitoring, etc.

When processing images from remote sensing systems, detection of spectral anomalies is relevant [3]. Qualitative detection of spectral anomalies makes it possible to further identify certain features of objects of interest and decipher the image.

Therefore, the task of detecting spectral anomalies in images from airborne remote sensing systems has been relevant.

Analysis of recent research and publications. In paper [3] the classification of optical-electronic systems for detection and identification of the image of objects according to their spectral features is given. three types of opto-electronic devices are consistently distinguished before classification.

The first type is a spectral anomaly detector that registers significant spectral differences between the pixels belonging to the search object and its surrounding neighborhood (background).

The second type of devices provides coordinated spectral filtering, which, with known spectral components of the search object and the background, performs spectral selection of the input signal with maximum suppression of background spectral components and minimal attenuation of spectral components belonging to the search object.

The third type of optical-electronic devices is designed to detect changes in the structure of two images. These devices detect the presence of changes in the structure of two images that are obtained at different points in time, or when comparing two images, one of which is a reference image and the other is the current image.

The task of detecting anomalies can also be interpreted as the task of image segmentation. Thus, in paper [4] the method of image segmentation from an unmanned aerial vehicle is considered. The main drawback of [4] is the failure to take into account spectral information regarding objects of interest.

Thus, the paper [5] considers the methods of distinguishing the boundaries of natural objects. Texture

recognition is performed using local binary patterns and digital wavelet transformation. The disadvantage of [5] is the application of the method only for a certain type of objects of interest and the limitation of the texture dictionary.

The paper [6] work developed a method of semantic segmentation of images from space surveillance systems. The method [6] is based on the use of convolutional neural networks, for example, modified U-net and RetinaNet architectures. The disadvantage of [6] is the segmentation of images with a certain type of objects of interest, for example, airplanes.

In the paper [7], the use of the TL-ResUNet architecture network is proposed for the segmentation of satellite images. The disadvantage of [7] is its use only for monitoring and analysis of agricultural land.

The paper [8] proposes a deep learning method for segmentation of the urbanized territory. The main drawback of [8] is its effectiveness only when segmenting an image of an urban area.

The paper [9] proposes a method of segmentation based on the algorithm of luminaries. The disadvantage of [9] is the difficulty of determining the objective function and the failure to take into account the spectral differences between the images of the objects of interest and the background.

The analysis of the dynamics of the object detection process by spectral features showed that at the initial stage of detection, when the spectral characteristics of the background are known, and the spectral characteristics of the search object are not known, it is advisable to use the anomaly detector.

Recently, a number of methods for detecting spectral anomalies have been created. However, none of them is optimal [10]. Therefore, the task of improving the method of detecting spectral anomalies, which provides improved characteristics, has been relevant.

From the analysis of known works, it can be concluded that there are two methods of detecting anomalies that are similar in their properties:

1. A calculation method that uses the Euclidean distance between different points. In relation to this problem, the Euclidean distance is a line segment that connects the ends of two random vectors that reflect the spectral properties of a surface area in three-dimensional space [11].

2. The Mahalanobis distance calculation method is a measure of the distance between vectors of random variables. Unlike the Euclidean distance, the Mahalanobis distance takes into account the correlation between variables and is scale invariant [12].

Based on the Mahalanobis distance, the anomaly detection algorithm proposed for processing spectral images in [13] is the RX-algorithm (RX detector). The value of the spectral difference calculated by the RX algorithm is the Mahalanobis distance to the average value of the spectral signatures in the image. Thus, signatures farthest from the average value, taking into account correlation dependencies between spectral channels, are considered anomalies. This algorithm demonstrated high results of processing images with a "simple" background, i.e. with one signature, but was ineffective for more complex tasks.

3. The method for calculating the contrast (brightness differences in three spectral channels) between the search object (potential anomaly) and the surrounding background is described in the paper [14].

4. The method based on Kullback-Leibler divergence is described in the paper [15]. It represents the information divergence (relative entropy), an asymmetric measure of the distance from each other of two probability distributions defined in the general space of elementary events [16]. Information about the separation of classes is contained mainly in the spectral distributions of optical signals, and its amount can be determined through the mutual information measure of statistical distributions - the Kullback-Leibler divergence. Information divergence (relative entropy) is a mathematical expectation of the likelihood ratio and is used in statistical processing tasks to divide two classes by the difference of their mathematical expectation and shows how much one distribution obeying the normal law differs from another.

Previously, the information criterion was used by the authors of this article as a measure of the consistency of optimal signal processing in electro-optical systems with dynamic spectral filtering [17-18], and in the paper [19] the information criterion was used to determine changes in the spectral structure of two images.

Thus, the **goal** of the article is to conduct a comparative analysis of methods for detecting spectral anomalies based on the calculation of the Euclidean distance, Mahalanobis distance, brightness contrast and Kullback-Leibler information divergence on images from airborne remote sensing systems.

Main results

1. ***Methods of detecting spectral anomalies of images.***

Each of the proposed methods includes the following operations:

First: a digital RGB image is formed as a result of registering the radiation of some object space [20]. According to the RGB color model, each element of color images with coordinates $(i,\ j)$ is represented as a vector

$$\vec{X}_{i,\ j} = \left[x_R(i,\ j),\ x_G(i,\ j),\ x_B(i,\ j) \right]^T$$

in three-dimensional Euclidean space, where x_R, x_G, x_B - brightness values measured in red (R-red), green (G-green) and blue (B-blue) spectral channels [21].

Secondly: the RGB image is conditionally divided into parts of the same size, which are given conventional designations (Fig. 1).

Third: the difference of each part of the image (potential anomaly) relative to another part of the image (potential background) is calculated.

The difference is calculated based on the indicators of spectral characteristics: the background mathematical expectation vector is calculated using the expression [22]:

$$\vec{\mu}_B = \frac{1}{b}\sum_{K=1}^{r} \vec{X}_K \,, \qquad (1)$$

where $\vec{X}_K$ – three-dimensional vector K-th element of a representative sample of the background; b – the number of elements of a representative sample of the background.

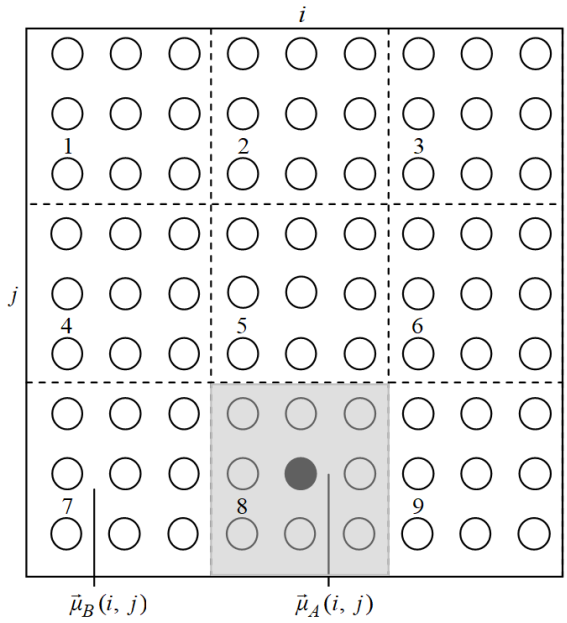

Fig. 1. The principle of detecting spectral anomalies of images

Accordingly, information about the spectral characteristics of the signal of the image section with the object of interest - a potential anomaly (vector of mathematical expectation of the anomaly) is calculated using the expression:

$$\vec{\mu}_A = \frac{1}{t}\sum_{A=1}^{r} \vec{X}_A \,, \qquad (2)$$

where $\vec{X}_A$ – three-dimensional vector A-th element of a representative sample of the image area with a potential anomaly; t – the number of elements of a representative sample of an image area with a potential anomaly.

The decision about the presence of a spectral anomaly in the area is made based on the highest indicator of the corresponding method

The image (Fig. 1) shows an illustration of the detection of a spectral anomaly (present on part No. 8). In the given example, the part for calculating the spectral characteristics of the conditional background consists of areas No. 1-7 and No. 9.

In case of determination of several areas with potential anomalies according to the highest indicators of the selected criteria, it is suggested to reduce the area of the image for analysis and carry out repeated calculations.

It should be noted that since all areas of the image except for the area with a hypothetical anomaly take part in the calculations of the indicators of the surrounding background, for the effective application of the considered methods, restrictions should be introduced - all elements of the surrounding background should be close in terms of spectral brightness. The cases of solving the following tasks may meet this condition: searching for an object in a field, searching for a surface object on the sea surface, searching for an object in a snowy area during a rescue operation, searching for an object of a certain color among multi-colored objects, etc.

Let's consider the mathematical foundations of the indicated methods of detecting spectral anomalies.

1.1. *A method for detecting spectral anomalies of images based on Euclidean distance calculation*.

The Euclidean distance is calculated using the expression [11, 23]:

$$D_e = \sqrt{\sum_{i=1}^{q}(x_i - y_i)^2} \,, \qquad (3)$$

where q – the number of characteristics; x_i, y_i – the vectors being compared.

Based on the condition of applying the Euclidean metric in the three-dimensional RGB space, we get that the Euclidean distance is a line segment that connects the ends of two vectors (potential anomaly and background) that reflect the spectral properties of the surface area in the three-dimensional space. Then the expression (3) for calculating the Euclidean distance will have the form:

$$D_e = \sqrt{(a_R - b_R)^2 + (a_G - b_G)^2 + (a_B - b_B)^2} \,, \qquad (4)$$

where a_R, a_G, a_B – brightness values of the vector of potential anomaly (vector of mathematical expectation of anomaly) $\vec{\mu}_{A_{i,\,j}} = [a_R(i,\ j), a_G(i,\ j), a_B(i,\ j)]^T$, which are measured in the red (R-red), green (G-green) and blue (B-blue) spectral channels the number of characteristics; b_R, b_G, b_B – brightness values of the background vector (mathematic expectation vector of the background) $\vec{\mu}_{B_{i,\,j}} = [b_R(i,\ j), b_G(i,\ j), b_B(i,\ j)]^T$, which are measured in the red (R-red), green (G-green) and blue (B-blue) spectral channels.

1.2. *The method of detecting spectral anomalies of images based on Mahalanobis distance calculation.*

The Mahalanobis distance is calculated using the expression [12]:

$$D_m = \sqrt{(\vec{\mu}_1 - \vec{\mu}_2)^T \Sigma^{-1} (\vec{\mu}_1 - \vec{\mu}_2)} \,, \qquad (5)$$

where $\vec{\mu}_1$ – multivariate vector to some distribution with mean vector $\vec{\mu}_2$ and common covariance matrix Σ.

Based on the condition of measuring the Mahalanobis distance in three-dimensional RGB space, the expression (5) will have the form:

$$D_m = \sqrt{(\vec{\mu}_A - \vec{\mu}_B)^T \Gamma^{-1} (\vec{\mu}_A - \vec{\mu}_B)} \,, \qquad (6)$$

where $\vec{\mu}_{A_{i,\,j}} = [a_R(i,\ j), a_G(i,\ j), a_B(i,\ j)]^T$ – three-dimensional potential anomaly vector to the distribution of the background signal (mathematical background expectation vector)

$$\vec{\mu}_{B_{i,\,j}} = [b_R(i,\,j), b_G(i,\,j), b_B(i,\,j)]^T$$

and common covariance matrix Γ of classes $\vec{\mu}_A$ and $\vec{\mu}_B$.

1.3. *The method of detecting spectral anomalies of images based on the calculation of the contrast (brightness differences in three spectral channels) of a potential anomaly relative to the background.*

The calculation of the contrast (brightness difference in three spectral channels) between the search object (potential anomaly) and the surrounding background is carried out using the expression [14, 24]:

$$C = (Y_T - Y_B)/(Y_T + Y_B), \qquad (7)$$

where Y_T, Y_B – the values of the target and the background signals.

Based on the condition of measuring the contrast of the potential anomaly relative to the surrounding background, the expression (7) will have the form:

$$C = \vec{F}_1^T \left(|\vec{\mu}_A - \vec{\mu}_B|\right) \Big/ \left(\vec{F}_1^T \left(\vec{\mu}_A + \vec{\mu}_B\right)\right), \qquad (8)$$

where $\vec{F}_1 = [1\ 1\ 1]^T$ – vector of the filter, which ensures the minimum attenuation of incoming radiation by the selecting device; $\vec{\mu}_T$, $\vec{\mu}_B$ – mathematical expectations of potential anomaly and background signals.

1.4. *The method of detecting spectral anomalies of images based on Kullback-Leibler information divergence.*

When solving the recognition task, the mathematical probability expectation for classes ω_A and ω_B is applied and the separation of classes is estimated by the difference of mathematical expectations [25]:

$$D = \int_{\Re} p\left(\vec{X}/\omega_A\right) \ln \frac{p\left(\vec{X}/\omega_A\right)}{p\left(\vec{X}/\omega_B\right)} d\vec{X} - \int_{\Re} p\left(\vec{X}/\omega_B\right) \ln \frac{p\left(\vec{X}/\omega_A\right)}{p\left(\vec{X}/\omega_B\right)} d\vec{X}, \qquad (9)$$

where $p\left(\vec{X}/\omega_A\right)$ – probability density of the accepted implementation in the presence of a class signal ω_A; $p\left(\vec{X}/\omega_B\right)$ – probability density of the accepted implementation in the presence of a class signal ω_B; $\ln p\left(\vec{X}/\omega_A\right) / p\left(\vec{X}/\omega_B\right)$ – likelihood ratios for classes ω_A and ω_B.

Assume that the accepted k-dimensional realizations are subject to the presence of class signals ω_A and ω_B obey the normal law with the corresponding probability densities:

$$p\left(\vec{X}/\omega_A\right) = N\left(\vec{\mu}_A, \Gamma_A\right); \qquad (10)$$

$$p\left(\vec{X}/\omega_B\right) = N\left(\vec{\mu}_B, \Gamma_B\right), \qquad (11)$$

where $\vec{\mu}_A$, $\vec{\mu}_B$ – mathematical expectations of classes ω_A and ω_B; Γ_A – covariance matrix of class ω_A; Γ_B – covariance matrix of class ω_B.

Using (9), we obtain the Kullback-Leibler divergence expression, which will have the following form:

$$D_{KL} = \frac{1}{2}\left[\begin{array}{l} \vec{\xi}^T \left(\Gamma_A^{-1} + \Gamma_B^{-1}\right)\vec{\xi} + \\ + tr\left(\Gamma_A \Gamma_B^{-1} + \Gamma_B \Gamma_A^{-1} - 2I\right) \end{array}\right], \qquad (12)$$

where $\vec{\xi} = \vec{\mu}_A - \vec{\mu}_B$ – vector of the difference of mathematical expectations of classes ω_A and ω_B; I – unit matrix; $tr(\bullet)$ – trace of the matrix; Γ_A – covariance matrix of class ω_A; Γ_B – covariance matrix of class ω_B.

2. ***Mathematical modeling of methods for detecting spectral anomalies of images.***

The purpose of mathematical modeling is a comparative assessment of the quality of methods for detecting spectral anomalies on images from airborne remote sensing systems.

2.1. *Mathematical modeling of methods for detecting spectral anomalies of images with a relatively "simple" background.*

First, let's assume that we have a color image with a spectral anomaly (Fig. 2), the size of which is 900×900 resolution elements (pixels). It shows a red square (spectral anomaly) on a green background.

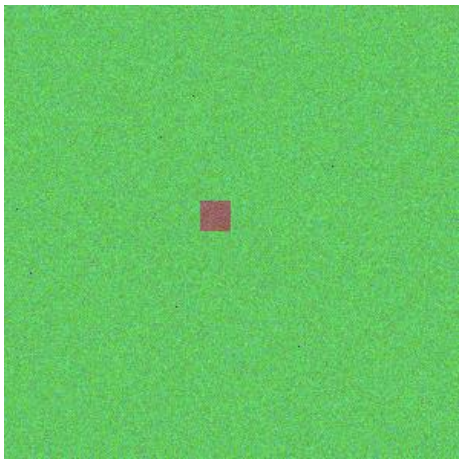

Fig. 2. RGB image under study

Secondly, the RGB image is conditionally divided into parts of the same size, which are given conventional designations (for example, into 9 identical parts) (Fig. 3).

Third: the difference of each part of the image (potential anomaly) relative to another part of the image (potential background) is calculated.

Using expression (4), the Euclidean distance of each part of the image (potential anomaly) relative to another part of the image (potential background) was calculated. The Fig. 4 shows a histogram of the calculated Euclidean distance of conditional parts of the RGB image under study.

According to the results of mathematical modeling, the decision about the presence of an anomaly (object of interest) should be made for part No. 5 (marked by the outline of a black square in Fig. 4) based on the largest Euclidean distance indicator: $D_e(№5) = 4,881$.

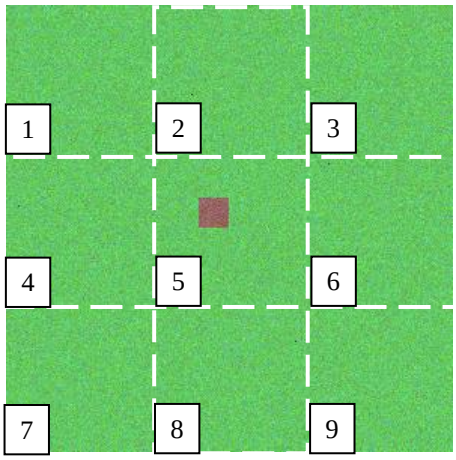

Fig. 3. The studied RGB image is divided into 9 identical parts with conventional designations

Using expression (6), the Mahalanobis distance of each part of the image (potential anomaly) relative to another part of the image (potential background) was calculated.

The Fig. 5 shows the histogram of the calculated Mahalanobis distance of conditional parts of the studied RGB image.

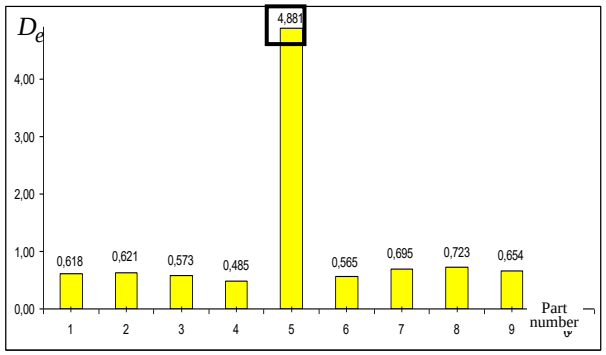

Fig. 4. The histogram is significantly different from the Euclidean conditional parts of the RGB image under study

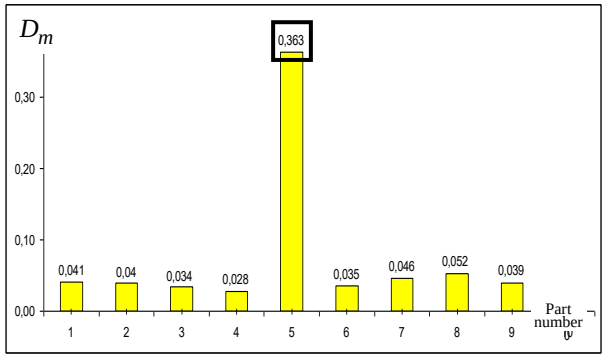

Fig. 5. The Histogram of the values of the Mahalanobis distance of conditional parts of the studied RGB image

According to the results of mathematical modeling, the decision about the presence of an anomaly (object of interest) should be made for part No. 5 (marked by the outline of a black square in Fig. 5) based on the largest Mahalanobis distance indicator:

$$D_m(№5) = 0,363.$$

Using expression (8), the calculation of the contrast of each part of the image (potential anomaly) relative to another part of the image (potential background) was performed. The Fig. 6 shows a histogram of the calculated contrast of conditional parts of the RGB image under study.

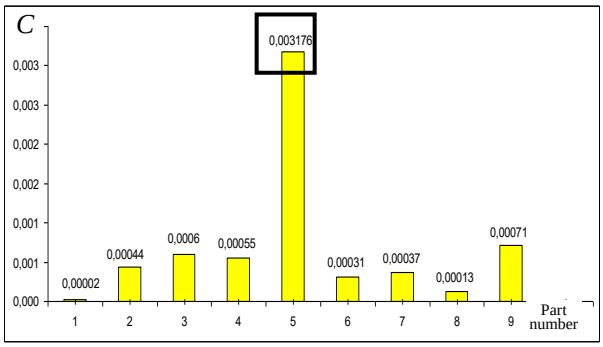

Fig. 6. The Histogram of contrast values of conventional parts of the studied RGB image

According to the results of mathematical modeling, the decision about the presence of an anomaly (object of interest) should be made for part No. 5 (marked by the outline of a black square in Fig. 6) based on the highest contrast index:

$$C(№5) = 0,003176.$$

Using expression (12), the Kullback-Leibler divergence of each part of the image (potential anomaly) relative to another part of the image (potential background) was calculated. The Fig. 7 shows a histogram of the calculated divergence of conditional parts of the RGB image under study.

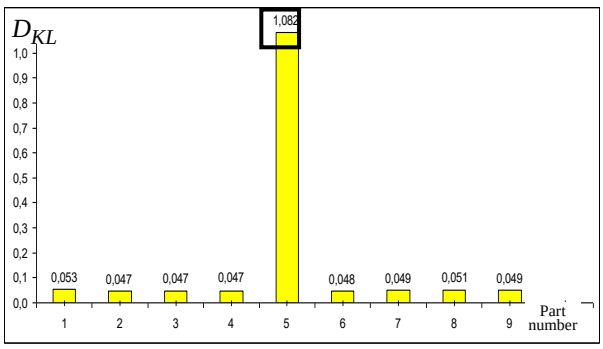

Fig. 7. The Histogram of divergence values Kulback-Leibler of conventional parts of the studied RGB image

According to the results of mathematical modeling, the decision about the presence of an anomaly (object of interest) should be made for part No. 5 (marked by the outline of a black square in Fig. 7) based on the largest divergence indicator:

$$D_{KL}(№5) = 1,082.$$

2.2. *Mathematical modeling of methods for detecting spectral anomalies of images with a complicated background.*

First, let's assume that there is a color image (Fig. 8), obtained from an aircraft in normal weather conditions using a digital camera, with a size of 840×1040 elements of resolution (pixels).

Fig. 8. RGB image under study

It shows a parking lot with a spectral anomaly (a yellow car) located on it. Secondly, the RGB image is conventionally divided into parts of the same size, which are given conventional designations (for example, into 16 identical parts) (Fig. 9).

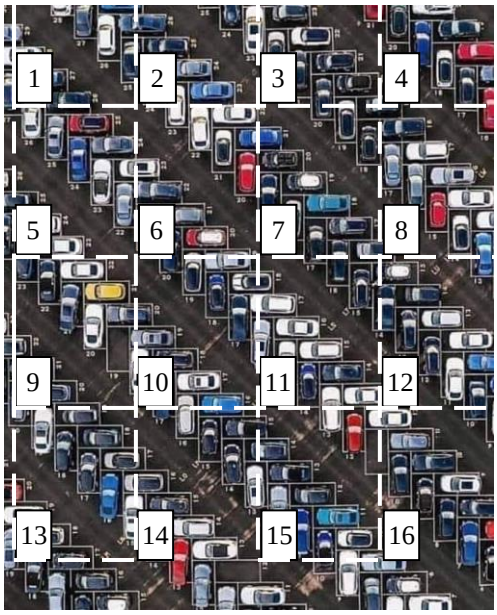

Fig. 9. The studied RGB image is divided into 16 identical parts with conventional designations

Third: the difference of each part of the image (potential anomaly) relative to another part of the image (potential background) is calculated.

Using expression (4), the Euclidean distance of each part of the image (potential anomaly) relative to another part of the image (potential background) was calculated. The Fig. 10 shows the histogram of the calculated Euclidean distance of the conditional parts of the studied RGB image.

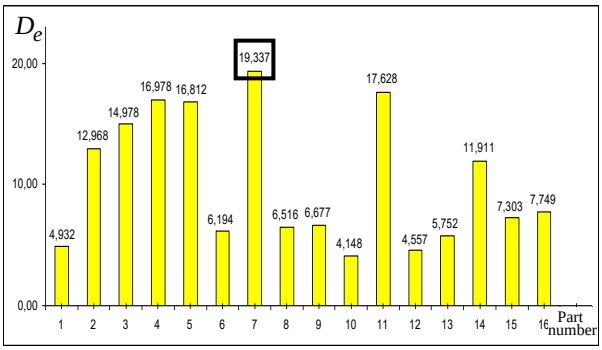

Fig. 10. The histogram is significantly different from the Euclidean conditional parts of the RGB image under study

According to the results of mathematical modeling, the decision about the presence of an anomaly (object of interest) should be made for part No. 7 (marked by the outline of a black square in Fig. 10) based on the largest Euclidean distance indicator: $D_e(№7) = 19,337$.

Using expression (6), the Mahalanobis distance of each part of the image (potential anomaly) relative to another part of the image (potential background) was calculated. The Fig. 11 shows the histogram of the calculated Mahalanobis distance of conditional parts of the studied RGB image.

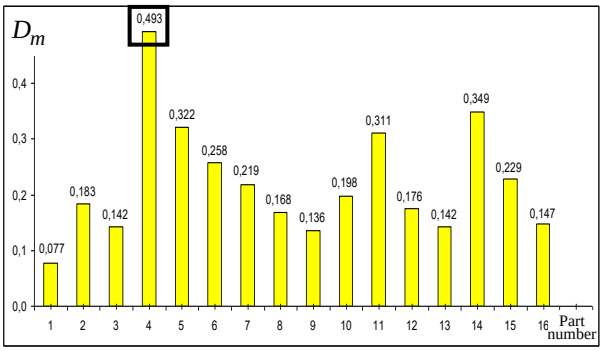

Fig. 11. The Histogram of the values of the Mahalanobis distance of conditional parts of the studied RGB image

According to the results of mathematical modeling, the decision about the presence of an anomaly (object of interest) should be made for part No. 4 (marked by the outline of a black square in Fig. 11) based on the largest Mahalanobis distance indicator: $D_m(№4) = 0,493$.

Using expression (8), the calculation of the contrast of each part of the image (potential anomaly) relative to another part of the image (potential background) was performed. The Fig. 12 shows a histogram of the calculated contrast of conditional parts of the RGB image under study.

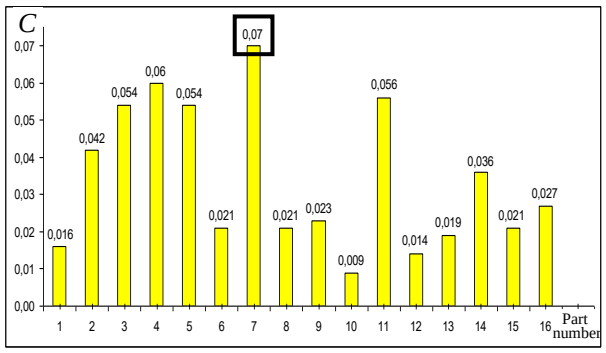

Fig. 12. The Histogram of contrast values of conventional parts of the studied RGB image

According to the results of mathematical modeling, the decision about the presence of an anomaly (object of interest) should be made for part No. 7 (marked by the outline of a black square in Fig. 12) based on the highest contrast index: $C(№7) = 0,07$.

Using expression (12), the Kullback-Leibler divergence of each part of the image (potential anomaly) relative to another part of the image (potential background) was calculated. The Fig. 13 shows a histogram of the calculated divergence of conditional parts of the RGB image under study.

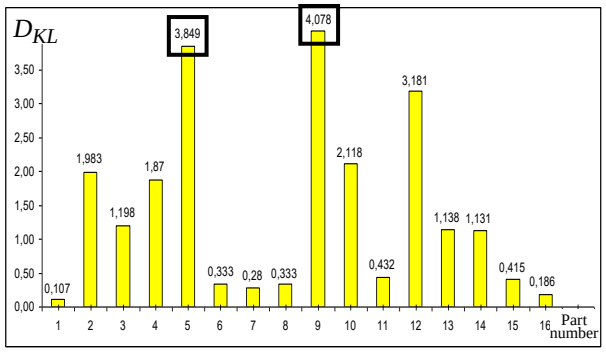

Fig. 13. The Histogram of divergence values Kulback-Leibler of conventional parts of the studied RGB image

According to the results of mathematical modeling, the decision about the presence of an anomaly (object of interest) should be made for parts No. 5 and No. 9 (marked by contours of black squares in Fig. 13) based on the largest divergence indicator:

$$D_{KL}(№5) = 3,849;$$

$$D_{KL}(№9) = 4,078.$$

In order to more accurately locate the spectral anomaly, since the method based on the Kullback-Leibler divergence is more effective than other methods when solving the task of finding a spectral anomaly on an image with a relatively complicated background, additional calculations of these parts should be performed. The Fig. 14 presents the investigated parts of the RGB image (No. 5 and No. 9) divided into 12 identical parts with conventional designations. Part No. 5 is divided into parts No. 51-56, and part No. 9 is divided into plots No. 91-96.

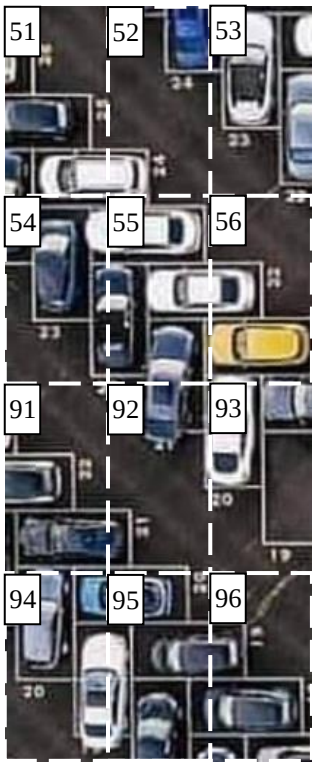

Fig. 14. The studied areas of the RGB image are divided into 12 identical parts with conventional designations

Using expression (4), the Euclidean distance of each part of the image (potential anomaly) relative to another part of the image (potential background) was calculated. The Fig. 15 shows the histogram of the calculated Euclidean distance of the conditional parts of the studied RGB image.

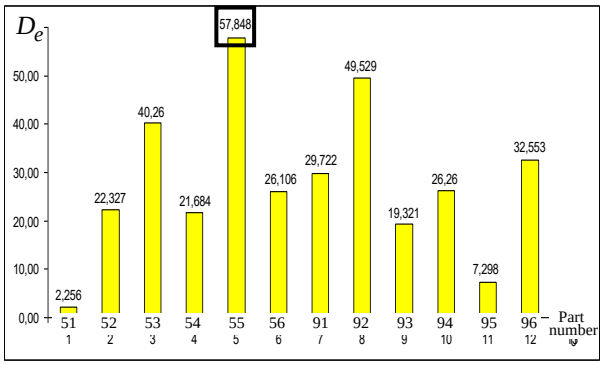

Fig. 15. The histogram is significantly different from the Euclidean conditional parts of the RGB image under study

According to the results of mathematical modeling, the decision about the presence of an anomaly (object of interest) should be made for part No. 55 (marked by the outline of a black square in Fig. 15) based on the largest Euclidean distance indicator:

$$D_e(№55) = 57,848.$$

Using expression (6), the Mahalanobis distance of each part of the image (potential anomaly) relative to another part of the image (potential background) was calculated.

The Fig. 16 shows the histogram of the calculated Mahalanobis distance of conditional parts of the studied RGB image.

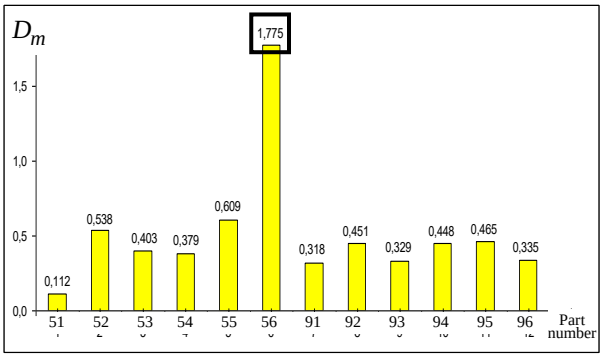

Fig. 16. The Histogram of the values of the Mahalanobis distance of conditional parts of the studied RGB image

According to the results of mathematical modeling, the decision about the presence of an anomaly (object of interest) should be made for part No. 56 (marked by the outline of a black square in Fig. 16) based on the largest Mahalanobis distance indicator:

$$D_m(№56) = 1,775 .$$

Using expression (8), the calculation of the contrast of each part of the image (potential anomaly) relative to another part of the image (potential background) was performed. The Fig. 17 shows a histogram of the calculated contrast of conditional parts of the RGB image under study.

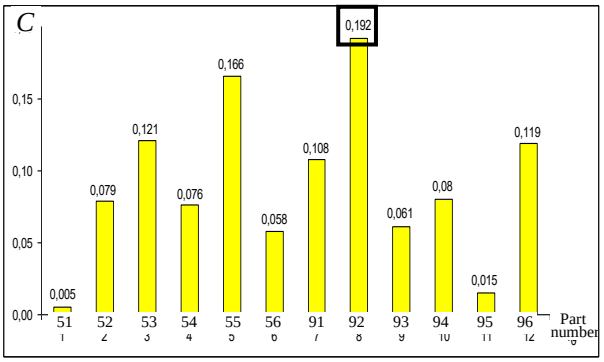

Fig. 17. The Histogram of contrast values of conventional parts of the studied RGB image

According to the results of mathematical modeling, the decision about the presence of an anomaly (object of interest) should be made for part No. 92 (marked by the outline of a black square in Fig. 17) based on the highest contrast index:

$$C(№92) = 0,192 .$$

Using expression (12), the Kullback-Leibler divergence of each part of the image (potential anomaly) relative to another part of the image (potential background) was calculated. The Fig. 18 shows a histogram of the calculated divergence of conditional parts of the RGB image under study.

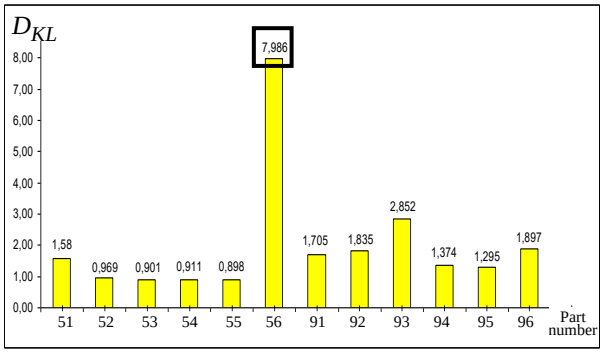

Fig. 18. The Histogram of divergence values Kulback-Leibler of conventional parts of the studied RGB image

According to the results of mathematical modeling, the decision about the presence of an anomaly (object of interest) should be made for part No. 56 (marked by the outline of a black square in Fig. 18) based on the largest divergence indicator:

$$D_{KL}(№56) = 7,986 .$$

So, after analyzing the results of mathematical modeling, the following conclusions can be drawn:

1. All the considered methods make it possible to search for a spectral anomaly in an image with a relatively simple background observed using an electro-optical system.

2. When searching for a spectral anomaly on an image with a complicated background, the Kullback-Leibler divergence method can be more effective than the other considered methods, but it is not optimal.

3. The application of the considered methods can provide both basic and additional information for determining areas for further analysis during the search for a spectral anomaly.

4. When determining several areas of the image with high divergence indicators, they should be investigated using the specified methods in order to more accurately determine the position of the spectral anomaly.

Conclusions and the directions of further research

The article is devoted to a comparative analysis of the effectiveness of methods for detecting spectral anomalies on images observed using an optical-electronic system. The main methods of detecting spectral anomalies on images from remote sensing systems were analyzed. Processing of images from remote sensing systems using the basic methods of detecting spectral anomalies was carried out. A comparative assessment of the quality of methods for detecting spectral anomalies on images from remote monitoring systems was carried out. It was established that the spectral difference of the considered methods is revealed by the value of information indicators - Euclidean distance, Mahalanobis distance, brightness contrast and Kullback-Leibler information divergence. Mathematical modeling of the considered methods of detecting spectral anomalies of images with a relatively "simple" and complicated background was carried out.

It was established that when searching for a spectral anomaly on an image with a complicated background, the method based on the Kullback-Leibler divergence can be more effective than the other considered methods, but is not optimal.

When determining several areas of the image with high divergence indicators, they should be additionally investigated using the specified methods in order to more accurately determine the position of the spectral anomaly.

REFERENCES

1. Sharad, W. (2021), "The development of the earth remote sensing from satellite", *Mechanics of gyroscopic systems*, No. 40 (2020), pp. 46–54, doi: https://doi.org/10.20535/0203-3771402020248768
2. Lafabregue, B., Gançarski, P., Weber, J. And Forestie, G. (2022), "Incremental constrained clustering with application to remote sensing images time series", *2022 IEEE International Conference on Data Mining Workshops* (ICDMW), pp. 814–823, doi: https://doi.org/10.1109/ICDMW58026.2022.00110
3. Eismann, M., Stocker, A. and Nasrabadi, N. (2009), "Automated hyperspectral cueing for civilian search and rescue", *2009 Proceedings of the IEEE*, vol. 97, no. 6, pp. 1031–1055, doi: https://doi.org/10.1109/JPROC.2009.2013561
4. Kumar, S., Kumar, A. and Lee, D.-G. (2022), "Semantic Segmentation of UAV Images Based on Transformer Framework with Context Information", *Mathematics*, vol. 10, no. 24, 4735, doi: https://doi.org/10.3390/math10244735
5. Favorskaya, M. N. and Zotin, A. G. (2021), "Semantic segmentation of multispectral satellite images for land use analysis based on embedded information", *Procedia Computer Science*, vol. 192, pp. 1504–1513, doi: https://doi.org/10.1016/j.procs.2021.08.154
6. Grosgeorge, D., Arbelot, M., Goupilleau, A., Ceillier, T. and Allioux R. (2020), "Concurrent segmentation and object detection CNNS for aircraft detection and identification in satellite images", *IEEE International Geoscience and Remote Sensing Symposium* (IGARSS), doi: https://doi.org/10.48550/arXiv.2005.13215
7. Safarov, F., Temurbek, K., Jamoljon, D., Temur, O., Chedjou, J. C., Abdusalomov, A. B. and Cho, Y. I. (2022), "Improved Agricultural Field Segmentation in Satellite Imagery Using TL-ResUNet Architecture", *Sensors*, vol. 22, no. 24, 9784, doi: https://doi.org/10.3390/s22249784
8. Neupane, B., Horanont, T. and Aryal J. (2021), "Deep Learning-Based Semantic Segmentation of Urban Features in Satellite Images: A Review and Meta-Analysis", *Remote Sensing*, vol. 13, no. 4, 808, doi: https://doi.org/10.3390/rs13040808
9. Khudov, H., Khizhnyak, I., Glukhov, S., Shamrai, N. and Pavlii V. (2024), "The method for objects detection on satellite imagery based on the firefly algorithm", *Advanced Information Systems*, vol. 8, no. 1, pp. 5–11. doi: https://doi.org/10.20998/2522-9052.2024.1.01
10. Borghys, D., Achard, V., Rotman, S.R., Gorelik, N., Perneel, C. and Schweicher E. (2011), "Hyperspectral anomaly detection: A comparative evaluation of methods", *XXXth URSI General Assembly and Scientific Symposium*, IEEE, pp. 1–4, doi: https://doi.org/10.1109/URSIGASS.2011.6050650
11. Redei, G. (2016), *Encyclopedia of Genetics, Genomics, Proteomics and Informatics*, Springer, Dordrecht, 638 p., doi: https://doi.org/10.1007/978-1-4020-6754-9_5603
12. Mclachlan, P. (1999), *Mahalanobis Distance / Resonance*, vol. 4, pp. 20–26, doi: https://doi.org/10.1007/BF02834632
13. Reed, I.S. and Yu, X. (1990), "Adaptive multiple-band CFAR detection of an optical pattern with unknown spectral distribution", *IEEE Transactions on Acoustics, Speech, and Signal Processing*, vol. 38, no. 10, pp. 1760–1770, doi: https://doi.org/10.1109/29.60107
14. Kupchenko, L., Rybiak, A., Goorin, O. and Biesova, O. (2022), "Experimental researches of dynamic spectral processing of optical radiation in the active electro-optical system", *Semiconductor Physics, Quantum Electronics & Optoelectronics*, vol. 25, no. 1, pp. 090–096, doi: https://doi.org/10.15407/spqeo25.01.090
15. Kupchenko, L., Khudov, H., Hurin, A., Rybiak, A. and Goorin O. (2022), "Improved method for detecting spectral anomalies based on the information criterion of Kulback-Leibler in remote sensing systems", *Weapon systems and military equipment*, vol. 2, no. 70, pp. 56–61, doi: https://doi.org/10.30748/soivt.2022.70.07
16. Kullback, S. and Leibler, R.A. (1951), "On information and sufficiency", The Annals of Mathematical Statistics, vol. 22, no. 1, pp. 79–86, doi: https://doi.org/10.1214/aoms/1177729694
17. Kupchenko, L. and Rybiak, A. (2015), "The matching criterion of optimal signal processing in electro-optical systems with dynamic spectral filtration", *Weapon systems and military equipment*, vol. 1, no. 41, pp. 120–123. URL: https://www.hups.mil.gov.ua/periodic-app/article/2504
18. Kupchenko, L., Rybiak, A. and Goorin O. (2018), "Estimation of matching of optimal dynamic spectral filtration in electro-optical system of target detection", Radiophysics and electronics, vol. 23, no. 1, pp. 42–52. doi: https://doi.org/10.15407/rej2018.01.042
19. Kupchenko, L., Khudov, H., Hurin, A., Rybiak, A. and Goorin, O. (2022), "Development of a method for detecting changes in the spectral structure of images using the information criterion – normalized Kullback-Leibler divergence", *Weapon systems and military equipment*, 2022, vol. 1, no. 69, pp. 33–39, doi: https://doi.org/10.30748/soivt.2022.69.04
20. Gorokhovatskyi, V., Peredrii, O., Tvoroshenko, I. and Markov, T. (2023), "Distance matrix for a set of structural description components as a tool for image classifier creating", *Advanced Information Systems*, vol. 7, no. 1, pp. 5–13, doi: http://dx.doi.org/10.20998/2522-9052.2023.1.01
21. Kuchuk, H., Kovalenko, A., Ibrahim, B.F. and Ruban, I. (2019), "Adaptive compression method for video information", *International Journal of Advanced Trends in Computer Science and Engineering*, vol. 8(1), pp. 66–69, doi: http://dx.doi.org/10.30534/ijatcse/2019/1181.22019
22. Tedore, C. and Johnsen, S. (2017), "Using RGB displays to portray color realistic imagery to animal eyes", *Current Zoology*, vol. 63, no. 1, pp. 27–34, doi: https://doi.org/10.1093/cz/zow076
23. Kovalenko, A. and Kuchuk, H. (2022), "Methods to Manage Data in Self-healing Systems", *Studies in Systems, Decision and Control*, vol. 425, pp. 113–171, doi: https://doi.org/10.1007/978-3-030-96546-4_3

24. Svyrydov, A., Kuchuk, H. and Tsiapa, O. (2018), “Improving efficienty of image recognition process: Approach and case study”, *Proceedings of 2018 IEEE 9th International Conference on Dependable Systems, Services and Technologies*, DESSERT 2018, pp. 593–597, DOI: https://doi.org/10.1109/DESSERT.2018.8409201·
25. Fukunaga, K. (1990), *Introduction to statistical pattern recognition*, Academic Press, Inc., San Diego, 626 p., doi: https://doi.org/10.1016/C2009-0-27872-X

Received (Надійшла) 20.03.2024
Accepted for publication (Прийнята до друку) 22.05.2024

ABOUT THE AUTHORS / ВІДОМОСТІ ПРО АВТОРІВ

Гурін Артем Петрович – ад’юнкт, Харківський національний університет Повітряних Сил імені Івана Кожедуба, Харків, Україна;
Artem Hurin – Post-Graduate Student, Ivan Kozhedub Kharkiv National Air Force University, Kharkiv, Ukraine;
e-mail: tema0504@gmail.com; ORCID ID: https://orcid.org/0000-0002-8536-4924;
Scopus ID: https://www.scopus.com/authid/detail.uri?authorId=58181599900

Худов Геннадій Володимирович – доктор технічних наук, професор, начальник кафедри тактики радіотехнічних військ, Харківський національний університет Повітряних Сил імені Івана Кожедуба, Харків, Україна;
Hennadii Khudov – Doctor of Technical Sciences, Professor, Head of Department of Radar Troops Tactic, Ivan Kozhedub Kharkiv National Air Force University, Kharkiv, Ukraine;
e-mail: 2345kh_hg@ukr.net; ORCID ID: https://orcid.org/0000-0002-3311-2848;
Scopus ID: https://www.scopus.com/authid/detail.uri?authorId=57196079841

Костиря Олександр Олексійович – доктор технічних наук, старший науковий співробітник, провідний науковий співробітник, Харківський національний університет Повітряних Сил імені Івана Кожедуба, Харків, Україна;
Oleksandr Kostyria – Doctor of Technical Sciences, Senior Researcher, Leading Reaearcher, Ivan Kozhedub Kharkiv National Air Force University, Ukraine;
e-mail: oleksandr.kostyria@nure.ua; ORCID ID: https://orcid.org/0000-0003-3363-2015;
Scopus ID: https://www.scopus.com/authid/detail.uri?authorId=37063443400

Масленко Олег Володимирович – кандидат технічних наук, старший дослідник, старший науковий співробітник науково-дослідного відділу, Науково-дослідний інститут воєнної розвідки, Київ, Україна;
Oleh Maslenko – PhD, Senior Researcher, Senior Researcher of Scientific Research Department, Defence Intelligence Research Institute, Ukraine;
e-mail: oleh.maslenko_1@gmail.com; ORCID ID: https://orcid.org/0000-0001-6963-6574;
Scopus ID: https://www.scopus.com/authid/detail.uri?authorId=58619026200

Сядристий Сергій Іванович – науковий співробітник, Харківський національний університет Повітряних Сил імені Івана Кожедуба, Харків, Україна;
Serhii Siadrystyi – Researcher, Ivan Kozhedub Kharkiv National Air Force University, Ukraine;
e-mail: siadristyi@ukr.net; ORCID ID: https://orcid.org/0009-0000-4875-6171.

Порівняльний аналіз методів виявлення спектральних аномалій на зображеннях з бортових систем дистанційного зондування

А. П. Гурін, Г. В. Худов, О. О. Костиря, О. В. Масленко, С. І. Сядристий

Анотація. Предметом вивчення в статті є методи виявлення спектральних аномалій на зображеннях з систем дистанційного зондування. **Метою** є проведення порівняльного аналізу методів виявлення спектральних аномалій на зображеннях з систем дистанційного зондування. **Завдання:** аналіз основних методів виявлення спектральних аномалій на зображеннях з систем дистанційного зондування; обробка зображень з систем дистанційного зондування основними методами виявлення спектральних аномалій; порівняльна оцінка якості методів виявлення спектральних аномалій на зображеннях з систем дистанційного моніторингу. Використовуваними **методами** є: методи цифрової обробки зображень, математичний апарат теорії матриць, методи математичного моделювання, методи теорії оптимізації, аналітичні та емпіричні методи порівняння зображень. Отримані такі **результати.** Проведено аналіз основних методів виявлення спектральних аномалій на зображеннях з систем дистанційного зондування. Проведена обробка зображень з систем дистанційного зондування основними методами виявлення спектральних аномалій. Проведена порівняльна оцінка якості методів виявлення спектральних аномалій на зображеннях з систем дистанційного моніторингу. **Висновки.** Спектральна відмінність розглянутих методів виявляється за значенням інформаційних показників – відстані Евкліда, відстані Махаланобіса, контрасту яскравості та інформаційної дивергенції Кульбака-Лейблера. Проведено математичне моделювання розглянутих методів виявлення спектральних аномалій зображень з відносно “простим” та ускладненим фоном. Встановлено, що при проведенні пошуку спектральної аномалії на зображенні з ускладненим фоном метод на основі дивергенції Кульбака-Лейблера може бути більш ефективним за інші розглянуті методи, але не є оптимальним. При визначенні декількох ділянок зображення з високими показниками дивергенції слід додатково їх дослідити із застосуванням визначених методів з метою більш точного визначення положення спектральної аномалії.

Keywords: спектральна аномалія; виявлення; дистанційне зондування; зображення; відстань Махаланобіса; контраст яскравості; дивергенція Кульбака-Лейблера.